Propulsive performance of a body with a traveling-wave surface

Fang-Bao Tian,[1,*] Xi-Yun Lu,[2] and Haoxiang Luo[1]
[1]*Department of Mechanical Engineering, Vanderbilt University, 2301 Vanderbilt Place, Nashville, Tennessee 37235-1592, USA*
[2]*Department of Modern Mechanics, University of Science and Technology of China, Hefei, Anhui 230026, China*
(Received 6 February 2012; published 6 July 2012)

A body with a traveling-wave surface (TWS) is investigated by solving the incompressible Navier-Stokes equation numerically to understand the mechanisms of a novel propulsive strategy. In this study, a virtual model of a foil with a flexible surface which performs a traveling-wave movement is used as a free swimming body. Based on the simulations by varying the traveling-wave Reynolds number and the amplitude and wave number of the TWS, some propulsive properties including the forward speed, the swimming efficiency, and the flow field are analyzed in detail. It is found that the mean forward velocity increases with the traveling-wave Reynolds number, the amplitude, and the wave number of the TWS. A weak wake behind the free swimming body is identified and the propulsive mechanisms are discussed. Moreover, the TWS is a "quiet" propulsive approach, which is an advantage when preying. The results obtained in this study provide a novel propulsion concept, which may also lead to an important design capability for underwater vehicles.

DOI: 10.1103/PhysRevE.86.016304 PACS number(s): 47.63.M−

I. INTRODUCTION

The mechanism of natural locomotion, including the flying of birds and insects and the swimming of fish and microorganisms, is a central issue for aerial and aquatic animals. Owing to the importance in fundamentals and applications, a great effort has been made in the past half century to study this subject, which has been widely reviewed [1–9].

Theoretical analyses were proposed typically for the low Reynolds number approximation and the high Reynolds number approximation regimes [10–12], which are known as Stokesian and Eulerian theories, respectively. The swimming of an infinite sheet, originally treated by the authors of Ref. [10] for the case of Stokes flow, was studied at moderate and high Reynolds numbers using the expansions by the authors of Refs. [13,14]. Fauci and Peskin [15] validated the equations in Refs. [10,13] by an immersed boundary method. It was found that the analytical equations are reliable at extremely low amplitude which is less than 2% of the wavelength. Teran *et al*. [16] found that for small amplitude, the numerical results can be recovered to the linear equations. Furthermore, they found that the result for finite length swimmers performing large tail undulations was substantially different from that of an infinite sheet with small amplitude undulations. The differences between undulating sheets of finite length and infinite length have been investigated by the authors of Refs. [17,18]. Recently, the linearized unsteady Navier-Stokes equation was solved in the frequency domain to study three-dimensional sheet executing spatially varying small amplitude oscillations in a viscous fluid [19]. Furthermore, the nonlinear equations of Stokesian dynamics were employed to analyze the swimming of animalcules in a viscous fluid at low Reynolds numbers [20]. However, numerous animals locomote in the range of the intermediate Reynolds number. In addition, the shape and the locomotion are complex for most animals. The mechanisms of locomotion appropriate to this Reynolds number range will no longer fall in the scope of either Stokesian or Eulerian or the linearized theory. Therefore, it is highly desirable to reveal the relevant mechanisms of locomotion based on some typical models.

Aquatic animals have evolved their superior performance of locomotion, which offers a paradigm of locomotion than that conventionally used in manmade vehicles. Recently, some novel propulsion ideas based on unsteady flow control have emerged as progress in robotics, smart materials, and control techniques. Using a flexible surface to produce a traveling wave, or traveling-wave surface (TWS), is a tool for unsteady flow control. The TWS might have been commonly produced by aquatic animals for tens of thousands years. For example, a series of skin waves on the bodies of a dolphin before lunging out of the water and swimming at high speed was observed [21]. We speculate that this mechanism might be used in nature and believe that the TWS control will have engineering applications as a result of the rapid development of smart materials and artificial muscles. A clue of this type of applications is implied in a recent study [22], which found that a cylinder with the downstream half made flexible to form an appropriate traveling transverse wave benefits by eliminating the vortex shedding and reducing the average drag. Although the skin waves were reported about half a century ago [21], the relevant mechanisms are still unclear, such as why this phenomenon exists and how it affects the swimming performance of aquatic animals, say dolphins. We will try to explain these questions in the present work by using numerical simulation.

The organization of the paper is as follows. The physical problem and mathematical formulation are described in Sec. II. The numerical results and discussion are presented in Sec. III, and finally, concluding remarks are provided in Sec. IV.

II. PHYSICAL PROBLEM AND MATHEMATICAL FORMULATION

In the present paper, a two-dimensional foil with a TWS is considered as the model of a free swimming body. As shown in Fig. 1, the vertical position of the top surface of the foil is described by

$$y_s(x,t) = y_{s0}(x) + y_{s0}(x)a_m \sin[2\pi k(x - ct)], \qquad (1)$$

*Corresponding author: fangbao.tian@vanderbilt.edu; onetfbao@gmail.com.

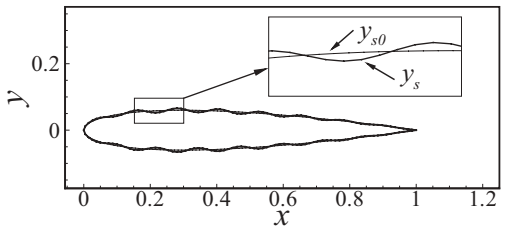

FIG. 1. The TWS of a two-dimensional model. The thin profile y_{s0} is the National Advisory Committee for Aeronautics (NACA)0012 foil and the thick profile y_s is the TWS generated along the surface of the foil. The insert is a close view of the difference between the foil surface and the TWS.

where $y_{s0}(x)$ is the profile of the foil, a_m is the ratio of the local amplitude of the TWS to the local half-width of the foil, k is the wave number, and c is the phase velocity. The motion of the bottom surface is obtained by considering the symmetry with respect to the central line of the body. Based on the active kinematics of the foil, the traveling-wave Reynolds number is defined as $\mathrm{Re}_c = \rho L c/\mu$, where L is the chord of the foil, ρ is the fluid density, and μ is the dynamic viscosity of the fluid. It should be pointed out that we recognize this model is somewhat limited. However, we still feel that the results will be of fundamental use in getting into the physical understanding of the mechanisms relevant to the TWS propulsion.

To simulate the free swimming of the foil with TWS, the space-time finite element method [23] is used to solve the two-dimensional incompressible Navier-Stokes equation, which has the following form:

$$\frac{\partial \boldsymbol{u}}{\partial t} + \boldsymbol{u}\cdot\nabla\boldsymbol{u} = -\nabla p + \nabla^2\boldsymbol{u}/\mathrm{Re}_c, \tag{2}$$

$$\nabla\cdot\boldsymbol{u} = 0, \tag{3}$$

where $\boldsymbol{u}$ is the velocity vector and p is the pressure. The details of the space-time finite element method can be found in Ref. [23] and a brief description is given here. In this method, the computations are carried out at one slice of the space-time domain between the time levels n and $n+1$. Therefore, a two-dimensional spatial problem is taken as a three-dimensional problem in the code including the time dimension. All the nodes of a slice are at time level n or $n+1$, and the spatial mesh at level $n+1$ can be different from that of level n and taken as a deformed version of the spatial mesh at level n. Hence, the moving mesh is achieved conveniently. The relevant code was extensively validated and verified to ensure the numerical accuracy and convergence in previous studies [17,24,25].

The thrust coefficient C_T (normalized by $\rho c^2 L/2$), due to the pressure and friction forces being exerted on the foil from the surrounding fluid, propels the foil to move horizontally by the relation

$$S\frac{d^2x_0}{dt^2} = -\frac{C_T}{2}, \tag{4}$$

where x_0 is the horizontal location of the foil and S is the mass ratio defined by $S = \rho_s A/\rho L^2$ with ρ_s and A being the density and area of the foil, respectively. Here, we simply take $\rho_s = \rho$.

III. RESULTS AND DISCUSSION

In this study, we will focus on the effects of kinematic parameters on the propulsive performance of TWS. These parameters are Re_c, a_m, and k. In the present work, $10^3 \leqslant \mathrm{Re}_c \leqslant 10^4$, $0.02 \leqslant a_m \leqslant 0.12$, and $2 \leqslant k \leqslant 8$.

A. Effect of Re_c

We first consider the effect of Re_c on the swimming performance of TWS at $a_m = 0.08$ and $k = 4$ by varying Re_c from 10^3 to 10^4. The simulations show that by performing TWS the body will swim forward. We denote the averaged forward velocity by $\bar{U}$. To measure the relation between c and $\bar{U}$, the swimming Reynolds number is defined as $\mathrm{Re}_U = \rho L\bar{U}/\mu$. The Re_c is used in the nondimensional governing equation of the fluid and Re_U can be obtained from $\mathrm{Re}_U/\mathrm{Re}_c = \bar{U}/c$ at the postprocessing calculation. The Re_c-Re_U relationship at $a_m = 0.08$ and $k = 8$ is shown in Fig. 2 involving several interesting observations. First, the ratio of the forward speed to the traveling-wave speed $\bar{U}/c$ varies from 0.24 to 0.54 and the limit of the ratio is 0.61 for the parameter regime considered, which is consistent with the results in the previous studies on undulatory swimming at moderate Reynolds number, for example, $\bar{U}/c \approx 0.48$ at $\mathrm{Re}_c = 1050$ by Dong and Lu [17] and $\bar{U}/c \approx 0.56$ at $\mathrm{Re}_c = 18\,300$ by Shen *et al.* [26]. It should be indicated that in real fish swimming, $\bar{U}/c$ could be larger than 0.6, as reported in Refs. [2,27]. Second, the forward speed increases with Re_c, which can be qualitatively explained as follows. For a steady forward swimming body, the force balance is described as $C_{Df} + 2H = C_T$, where C_{Df} is the friction drag coefficient defined by the forward speed and proportional to $\mathrm{Re}_c^{-1/2}$, $2H$ is the drag coefficient calculated by the free stream theory [28] and independent of Re_c, and C_T is the pressure thrust by the traveling wave and is an increasing function of $(c^2 - \bar{U}^2)/c^2$ [29]. Thus, when Re_c is increased, C_{Df} decreases and consequently C_T decreases, resulting in $(c^2 - \bar{U}^2)/c^2$ being depressed or the forward speed being increased. Finally, the Re_c-Re_U curve is linear at larger

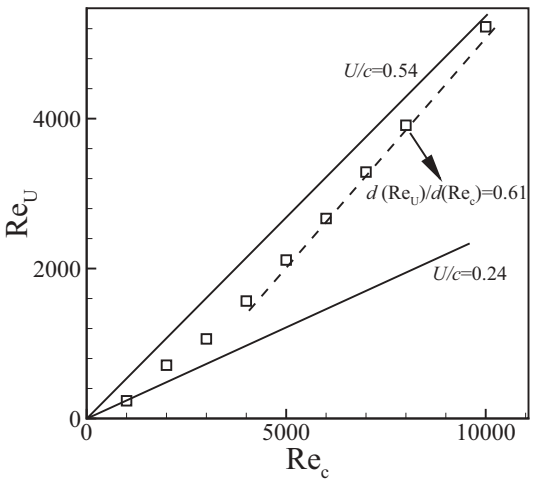

FIG. 2. The relationship between the traveling-wave Reynolds number and swimming Reynolds number at $a_m = 0.08$ and $k = 8$. $\mathrm{Re}_U/\mathrm{Re}_c = \bar{U}/c$ varies from 0.24 to 0.54 and the limit of the ratio is 0.61 for the parameter regime considered.

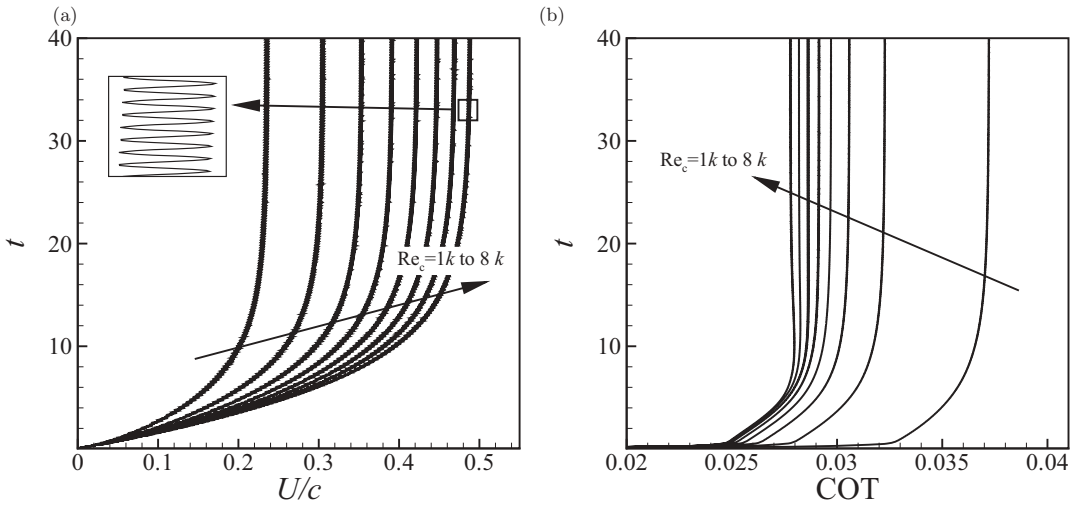

FIG. 3. The propulsive performance of the TWS at $a_m = 0.08$ and $k = 8$. (a) The forward swimming speed. (b) COT.

Re_c, as $\mathrm{Re}_c > 5000$, which can be explained as follows. When $\mathrm{Re}_c \to \infty$, the force balance is $2H = C_T$. It is known that $2H$ is independent of Re_c and C_T is a function of $\bar{U}/c$. Thus, to keep the force balance, $\bar{U}/c$ must be a constat at large Re_c; this ratio is 0.61 in the present simulation.

To discuss the propulsive performance of the TWS, we define the costs of transport (COT, which means energy required to transport 1 N over 1 m) as $C = P/WU$ [2], where P is the total power for swimming which is obtained by the integral of the inner product of the hydrodynamic force and velocity [17] and W is the weight of the fish model. The velocities and COTs at different Re_c are shown in Fig. 3. It is found that during the initial acceleration phase, the body with higher Re_c is accelerated faster than that with lower Re_c. The accelerations, the final speeds and COTs at large Re_c get close to their limits. COT is smaller for larger Re_c which means the efficiency at larger Re_c is higher. Furthermore, the forward swimming speeds are close to other propulsive methods [2,30–32], while COTs are lower compared to the data reported in Ref. [2]. To explain this finding, note that for large Re_c the viscous force is small enough to be ignored. On the other hand, the viscous effect on the TWS boundary makes the forward speed smaller for the smaller Re_c and the pressure distribution on the surface is shifted. Thus, the parts of power used to overcome the pressure due to the formation of traveling-wave and shear stresses are decreased when Re_c is increased, and consequently the forward speed is increased and the COT is decreased. Similar results are implied in the previous study for the undulatory swimming [32].

B. Effect of k and a_m

To further investigate the role of kinematics on swimming performance, the simulations are performed for a certain k (or a_m) with changing a_m (or k). The results are shown in Fig. 4. It is found that Re_U (or forward swimming speed) is a

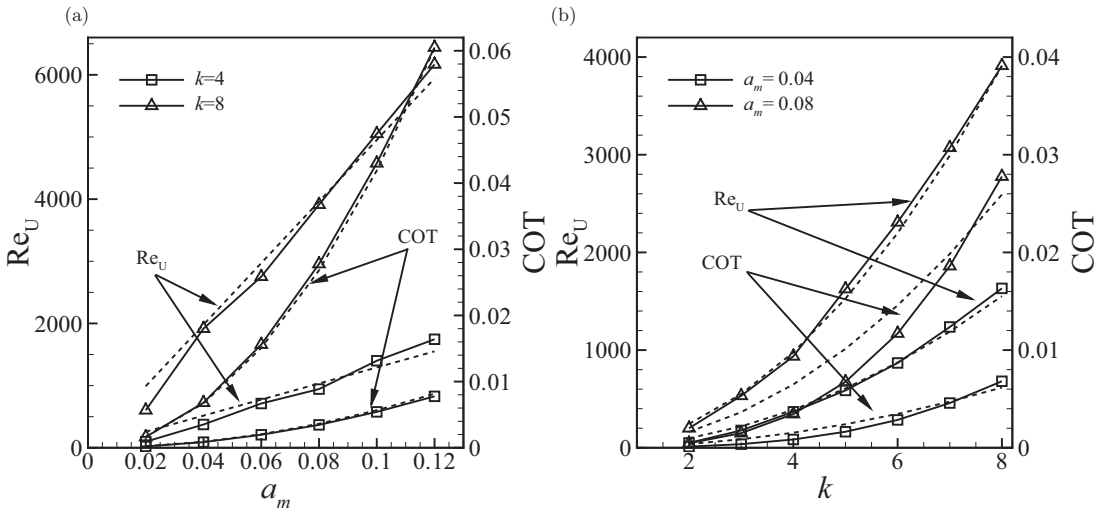

FIG. 4. Role of kinematics on swimming performance at $\mathrm{Re}_c = 8000$. (a) a_m–Re_U and COT at $k = 4$ and 8. (b) k–Re_U and COT at $a_m = 0.04$ and 0.08. The dashed lines in (a) are the first-order approximations for Re_U and first-order approximations for COT, and in (b) are the second-order approximations for both Re_U and COT.

monotone increasing function of a_m(or k) for a certain k (or a_m). In addition, the forward swimming speed is approximately first order of a_m and second order of k (as demonstrated in Fig. 4 by the dashed lines), which is different from that of an infinite sheet [13,14,33,34]. Comparably, the forward speed of an infinite sheet is the second order of the amplitude and wave number. Their difference is understandable considering the infinite length and uniform waving amplitude used in the previous references, while the finite length and nonuniform amplitude are applied in the present study. The other interesting observation from Fig. 4 is that COT is the second order of the amplitude and wave number. Correspondingly, COT increases with amplitude and wave number and thus the swimming efficiency at smaller amplitude and wave number is higher. Compared to the data reported in Ref. [2], the COT of TWS propulsion is smaller than most swimmers ($\geqslant$0.1), which means that the efficiency of TWS propulsion is higher. In Ref. [2] only *Eschrichtius robustus* has a comparative COT, which is 0.04. It should be noted that the metabolic rate used to calculate COT for real fish include the efficiency of muscles (not more than 50%) and also all the energy spent for other biological processes. Nevertheless, the equivalent COT of TWS propulsion (divide COT in Fig. 4 by $0.4 \sim 0.5$) is still smaller than most swimmers.

The advantage of the TWS is obvious when we rescale the results in Fig. 4 based on the approach summarized in Ref. [35]. The forward speed $\bar{U}/c$ as a function of $\pi A_0 k$ ($A_0 = 0.12a_m$ being the maximal amplitude) is shown in Fig. 5, where the results for an infinite sheet predicted by the authors of Ref. [13] and finite swimming foils adapted from Refs. [30, 31,36] are presented for comparison. As we can see from Fig. 5, the forward speed of the TWS is larger than other propulsion methods. It is noted that the speed of the infinite sheet predicted by the authors of Ref. [13] is much smaller than those of finite swimming foils, including the present results. The results imply that the analytical equation of the infinite sheet underestimates the forward swimming speed.

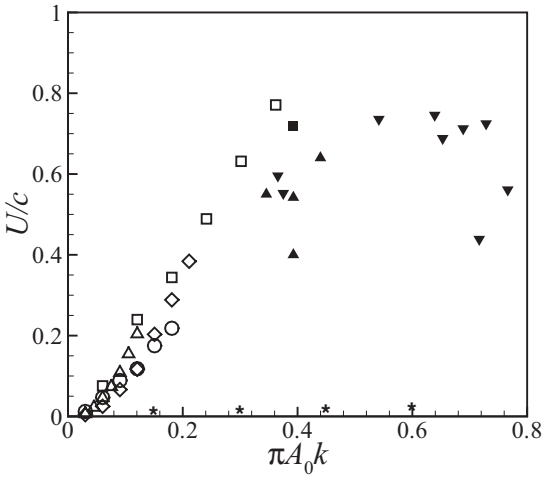

FIG. 5. Rescaled propulsive performance shown in Fig. 4: ◯ for $k = 4$, changing a_m; □ for $k = 8$, changing a_m; △ for $a_m = 0.04$, changing k; ◇ for $a_m = 0.08$, changing k; ■ for results adapted from Ref. [30]; ▲ for results adapted from Ref. [31]; ▼ for results adapted from Ref. [36]; ∗ for the results predicted by Ref. [13].

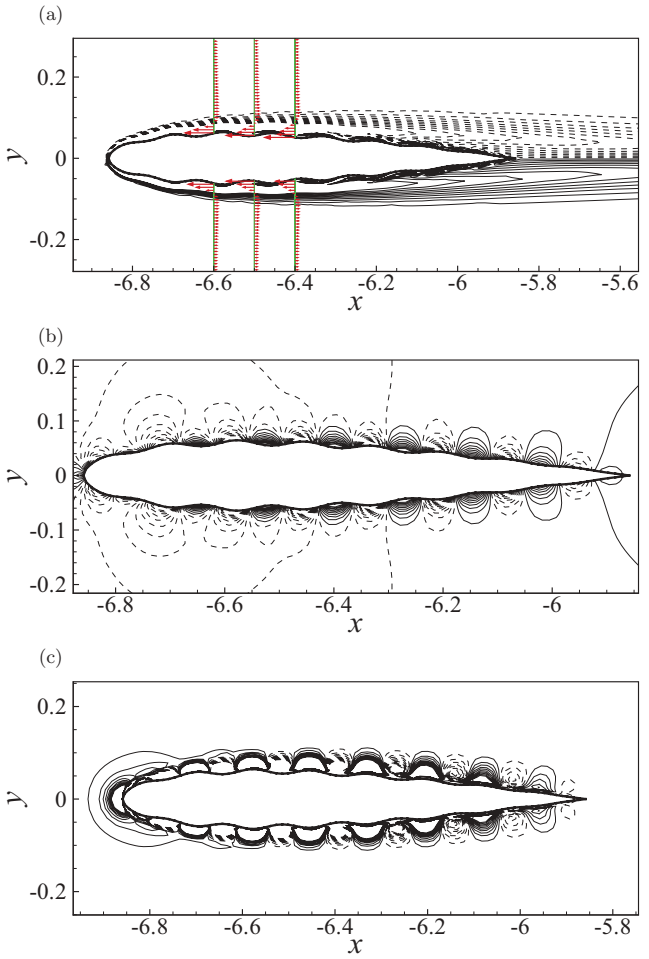

FIG. 6. (Color online) Flow fields for $\mathrm{Re}_c = 8000$, $a_m = 0.08$, and $k = 8$. (a) Vorticity, (b) pressure, and (c) acoustic source. The red vector in (a) shows the u profile along y.

C. Flow field

The instantaneous fields of vorticity, pressure, and acoustic source are shown in Fig. 6 from which several interesting observations are obtained. First, there is no vortex street in the wake generated by the TWS, which is a drag-producing wake, as shown in Fig. 6(a). On the other hand, the reverse Kármán vortex street, known as a thrust-producing wake, is commonly observed in fish-like locomotion or flapping wing flight [37]. Second, it is noted that there is a backward jet outside the shear layer, as shown in Fig. 6(a). Therefore, the thrust is generated by the jet outside the boundary and the high pressure on the leeward side of the traveling wave, as demonstrated in Figs. 6(a) and 6(b). The jet outside the boundary layer cannot be predicted by the linear analytical equation for an infinite sheet [13], which may be the major cause of the difference between the swimming speeds of TWS and the infinite sheet with small amplitude. Finally, the acoustic source calculated by $\nabla \cdot (\mathbf{u} \cdot \nabla \mathbf{u})$ [38] shows that it is mainly distributed near the TWS rather than in the wake, as shown in Fig. 6(c). In contrast, for the propulsion by the thrust-producing wake, the acoustic source is mainly generated in the wake of the reverse Kármán vortex street. Therefore, TWS can be regarded as a

"quiet" propulsive strategy from which aquatic animals can get benefits when preying [39].

IV. CONCLUDING REMARKS

Based on numerical analysis on a virtual model, we have found that the body subjected to the traveling-wave surface moves spontaneously in the horizontal direction. The mean forward velocity increases with the traveling-wave Reynolds number, as well as the amplitude and wave number of the traveling wave. The forward speed of TWS is much higher than other propulsion methods, and the propulsive efficiency is larger than most aquatic animals. Moreover, it is found that there is no vortex street in the wake of the body and thrust is generated by the backward jet outside the boundary layer and the high pressure on the leeward side of the traveling wave. Furthermore, the acoustic source is mainly distributed near the TWS boundary and thus the TWS acts as a "quiet" propulsive strategy.

ACKNOWLEDGMENTS

We appreciate the anonymous reviewer for bringing us to use COT as the measurement of swimming efficiency. This work was supported by the National Natural Science Foundation of China (No. 10832010), the Innovation Project of the Chinese Academy of Sciences (No. KJCX2-YW-L05), and the United States National Science Foundation (No. CBET-0954381).

[1] M. J. Lighthill, Annu. Rev. Fluid Mech. **1**, 413 (1969).
[2] J. J. Videler, *Fish Swimming* (Chapman and Hall, London, 1993).
[3] M. S. Triantafyllou, G. S. Triantafyllou, and D. K. P. Yue, Annu. Rev. Fluid Mech. **32**, 33 (2000).
[4] T. Y. Wu, Adv. Appl. Mech. **38**, 291 (2001).
[5] Z. J. Wang, Annu. Rev. Fluid Mech. **37**, 183 (2005).
[6] F. E. Fish and G. V. Lauder, Annu. Rev. Fluid Mech. **38**, 193 (2006).
[7] W. Shyy, H. Aono, S. K. Chimakurthi, P. Trizila, C. K. Kang, C. E. S. Cesnik, and H. Liu, Progr. Aerospace Sci. **46**, 284 (2010).
[8] E. D. Tytell, I. Borazjani, F. Sotiropoulos, T. V. Baker, E. J. Anderson, and G. V. Lauder, Integ. Comp. Biol. **50**, 1140 (2010).
[9] T. Y. Wu, Annu. Rev. Fluid Mech. **43**, 25 (2011).
[10] G. Taylor, Proc. R. Soc. London A **209**, 447 (1951).
[11] M. J. Lighthill, *Biofluiddynamics* (Society for Industrial and Applied Mathematics, Philadelphia, 1975).
[12] S. Childress and R. Dudley, J. Fluid Mech. **498**, 257 (2004).
[13] E. O. Tuck, J. Fluid Mech. **31**, 305 (1968).
[14] S. Childress, ASME Conf. Proc. **2008**, 1413 (2008).
[15] L. J. Fauci and C. S. Peskin, J. Comput. Phys. **77**, 85 (1988).
[16] J. Teran, L. Fauci, and M. Shelley, Phys. Rev. Lett. **104**, 038101 (2010).
[17] G. J. Dong and X. Y. Lu, Int. J. Numer. Methods Fluids **48**, 1351 (2005).
[18] X. Y. Lu and X. Z. Yin, Acta Mech. **175**, 197 (2005).
[19] C. A. Van Eysden and J. E. Sader, Phys. Fluids **18**, 123102 (2006).
[20] B. U. Felderhof, Phys. Fluids **18**, 063101 (2006).
[21] H. Hertel, *Structure, Form, Movement* (Reinhold, New York, 1966).
[22] C. J. Wu, L. Wang, and J. Z. Wu, J. Fluid Mech. **574**, 365 (2006).
[23] T. E. Tezduyar, M. Behr, S. Mittal, and J. Liou, Comput. Meth. Appl. Mech. Engrg. **94**, 353 (1992).
[24] G. J. Dong and X. Y. Lu, Phys. Fluids **19**, 057107 (2007).
[25] S. Y. Wang, F. B. Tian, L. B. Jia, X. Y. Lu, and X. Z. Yin, Phys. Rev. E **81**, 036305 (2010).
[26] L. Shen, X. Zhang, D. K. P. Yue, and M. S. Triantafyllou, J. Fluid Mech. **484**, 197 (2003).
[27] C. Eloy, J. Fluids Struct. **30**, 205 (2012).
[28] G. K. Batchelor, *An Introduction to Fluid Dynamics* (Cambridge University Press, Cambridge, England, 1967).
[29] M. J. Lighthill, J. Fluid Mech. **9**, 305 (1960).
[30] J. Carling, T. L. Williams, and G. Bowtell, J. Exp. Biol. **201**, 3143 (1998).
[31] S. Kern and P. Koumoutsakos, J. Exp. Biol. **209**, 4841 (2006).
[32] I. Borazjani and F. Sotiropoulos, J. Exp. Biol. **213**, 89 (2010).
[33] S. Childress, *Mechanics of Swimming and Flying* (Cambridge University Press, New York, 1981).
[34] M. Sauzade, G. J. Elfring, and E. Lauga, Physica D **240**, 1567 (2011).
[35] A. Azuma, *The Biokinetics of Flying and Swimming* (AIAA, Reston, VA, 2006), 2nd ed.
[36] E. D. Tytell, C. Y. Hsu, T. L. Williams, A. H. Cohen, and L. J. Fauci, Proc. Natl. Acad. Sci. USA **107**, 19832 (2010).
[37] D. S. Barrett, M. S. Triantafyllou, D. P. K. Yue, M. A. Grosenbaugh, and M. J. Wolfgang, J. Fluid Mech. **392**, 183 (1999).
[38] M. J. Lighthill, Proc. R. Soc. London A **211**, 564 (1952).
[39] J. M. Moulton, Biol. Bull. **119**, 210 (1960).